Reprinted from the Preprint Volume of the Tenth Conference on Biometeorology and Aerobiology and the Special Session on Hydrometeorology, September 10-13, 1991, Salt Lake City, Utah. Published by the American Meteorological Society, Boston, Mass.

J3.2

A STUDY OF THE MECHANISM AND IMPACT OF BIOSPHERE FEEDBACK ON THE AFRICAN CLIMATE

Y. Xue and J. Shukla

Center for Ocean–Land–Atmosphere Interactions (COLA)
Department of Meteorology
University of Maryland
College Park, Maryland 20742

1. INTRODUCTION

The semiarid areas of Sahel is the zone between the Sahara desert and the savannah lands to the south. It is characterized by the strong seasonality of the climate with a short rainy season in northern summer. According to Nicholson (1980) and Lamb's (1985) studies there were several drought periods in African history, followed by the wet episodes. Since late 1960s, an extensive drought swept across the Sahel and Ethiopia. The drought has lasted about 20 years and so far there is no sign of the end of the drought situation. Current research on this problem has focused either on the influence of sea surface temperature (SST) or land–surface changes. We focus on the land surface effects in this paper.

According to Skoupy (1987) and Lanly's (1982) study, for a half century, and particularly over the past 30 years, the plant cover in Africa has been increasingly degraded across the African continent. Such large scale land surface destruction may have a significant impact on the African climate. Meteorologists have long suspected a relationship between desertification and African drought (Charney, 1975; Walker and Rowntree, 1977; Shukla and Mintz, 1982; Sud and Smith, 1984; Xue et al., 1990). In this study, we try to simulate the effect of the desertification on African drought using a realistic model of atmosphere–biosphere.

2. MODEL DESCRIPTION

The GCM model being used in this study is a modified version of the National Meteorological Center (NMC) global spectral model (GCM). The detailed formulation and the initialization procedures and boundary conditions are described in Sela (1980) and Kinter et al. (1988). An interactive cloud scheme, which is similar to the one developed by Slingo (1987), was incorporated in the GCM (Hou, 1990).

The biosphere model used in this study was developed by Xue et al. (1991) which is a simplified version of Simple Biosphere Model (SiB) of Sellers et al. (1986). There are three major parts in SiB: calculation of radiative transfer at surface, aerodynamic resistances, and stomatal resistances. All three parts are simplified in the current version.

There are twelve vegetation types in the SiB model. Different biomasses are distinguished by vegetation and soil parameters. Four types have two vegetation layers in the original SiB model. The Sahel area is covered by two two–layer vegetation types. The second layer covers whole ground like a lid. This type of structure has yet to be verified with the observational data. We eliminated the ground cover and re–optimized the vegetation parameters. While the second layer was eliminated, the properties of the two layers are combined into a set of reconstructed parameters consisting of one layer each. In this way, we also reduce the total number of parameters used in this model.

3. EXPERIMENTAL DESIGN OF DESERTIFICATION AND AFFORESTATION

Dregne (1977) compiled a map to show the status of desertification in each continent. He divides the degree of desertification into four classes: slight, moderate, severe, and very severe. The Sahel region is categorized as a severe desertification region on this map. In our model, the changes of the vegetation types have been used to describe the degradation of the plant and soil.

There are four vegetation types in North Africa in the SiB model: bare soil (vegetation type 11), broadleaf shrub with bare soil (type 9), broadleaf shrub with ground cover (type 8), and broadleaf trees with ground cover (type 6). The Sahara desert consists of types 9 and 11 (Fig. 1a).

Table 1 shows the values of some vegetation and soil parameters for types 6, 8, 9, and 11.

From Table 1, we can find that type 6 has larger vegetation cover, leaf index, greenness, and surface roughness length than type 9; it has loam soil. Type 8 and type 9 both have sandy soil, which has less capacity to hold water. Type 8 has larger leaf index and surface roughness than type 9.

Due to lack of vegetation data after desertification in Sahel region, we simply replace the vegetation types 6 and 8 in that region with type 9. This reduces the vegetation cover, leaf index, roughness length, soil depth, and degrades other vegetation and soil properties. Figure 1a shows the original vegetation types in SiB model over Africa. Figure 1b shows the vegetation types after desertification. It covers Dragne's severe desertification area, but expanded to the southwest. This area is from about 10° N to 18.5° N.

Although we use type 9, not type 11 to describe the desertification, the changes we made here still exaggerate the real desertification.

The surface albedo changes with the vegetation type. The albedo varies with a diurnal variation in the SiB model. The mean value of the albedo is about 0.3 for desert, and about 0.2 for vegetation types 6 and 8. The albedo changed by about 0.10 after the vegetation was altered.

We also designed an afforestation experiment, to test the impact of large scale revegetation on the Sahel climate. Since afforestation experiment is a pure sensitivity study, we do not reconstruct new vegetation types, but simply chose type 6 to replace types 8 and 9. The afforestation area is depicted in Fig. 1c and spans about 7° of latitudes. The albedo lowers by about 0.1. Since type 8 and type 6 have almost the same albedo, the albedo change area is smaller than that in the desertification experiment.

4. EXPERIMENTS AND DATA

We used different SSTs and initial conditions in our experiments. The rainy season in sub–Sahara area lasts about 2–5 months during boreal summer (Nicholson, 1980). We started our model integrations from June and integrated for three months to have a larger response from the anomaly experiments. All model integrations were started from the initial conditions of June 1 or June 2, 1988. According to observations, 1988 had the highest precipitation rate during the 1980s. June 1, 1987, which was relatively dry, also was used as one of the initial conditions.

We obtained SST data sets from the U.K. Meteorology Office for boundary condition, which include 1950, 1983, and climatological SST. It is prescribed in the model and updated once a day in our numerical experiments.

We conducted one control experiment and two anomaly experiments (desertification and afforestation) in this study. Each experiment consisted of five cases, which had different initial and/or boundary conditions. Three of them used climatological SST as boundary condition with June 1, 1988, June 2, 1988, and June 1, 1987 as the initial conditions. We also used 1983 SST and 1950 SST, since 1950 is the wettest year in Africa during this century and 1983 is the second driest year.

Table 2 shows the cases in our experiments. We denote control experiments by C, desertification experiment by D and afforestation experiment as A in the rest of the text.

The soil moisture also has to be changed in anomaly cases. The soil wetness became about 0.05 in the test area in Cases D and about 0.16 in Case R.

5. RESULTS FROM DESERTIFICATION EXPERIMENTS

Due to the large amount of computing time required by these experiments, we run our experiments in NASA CRAY YMP, NCAR CRAY XMP and YMP. All these cases were integrated for ninety days.

Figures 2a–c show the five case mean rainfall over Africa for Case D, Case C, and difference (D–C). From Fig. 2c, we find that, after desertification, the rainfall reduced more than 1 mm/day and there is a clear dipole pattern. The rainfall reduced in the desertification area. But it increased slightly in the south of this region. According to Nicholson's studies (1981), rainfall anomalies frequently occur of opposite sign north and south of 10°N, with the discontinuity at this latitude being very sharp.

Another important feature is the displacement of isohyets. The isohyets moved south in the desertification experiment.

Figure 3 has the time series of the rainfall for Case C2 and D2, which is based upon daily means over the test area. This figure (and other cases) showed that the rainfall drop in the desertification experiment started from about the third day and continued, throughout whole period. We had similar results for other cases.

For the afforestation experiment, we had the similar results, but with the opposite sign. Figures 4a,b show five case mean rainfall for afforestation and difference between afforestation and control Case (A–C). The impact was not as large as in the desertification experiment. The afforestation area in this case is less than that in Case D. It is also possible that the location of the changed surface condition is closer to the descending branches of the tropical Hadley circulation in Case A. The rainfall increased about 1 mm/day in the test region.

6. THE ANALYSIS OF THE HYDROLOGICAL-CYCLE AND RADIATION BUDGET

Figures 5–7 show the accumulative rainfall, evaporation from surface, and surface runoff. Figure 8 is total soil water content at ground. All these results are from Cases C2 and D2 for test area. After desertification the rainfall was reduced by 107 mm during 90 days. However, despite the reduced rainfall, the surface runoff increased by about 60 mm. This is because less rain was intercepted by leaves and a large portion of the precipitation would directly hit the ground. Meanwhile, the soil layer had less capacity to hold water in desert area. The evaporation reduced by about 60 mm in that period. This amount of reduction is not large enough to compensate the deficit caused by the reduced rain and enhanced runoff. The total soil water content was reduced by 107 mm in the desertification area.

We find that the reduction of rainfall and evaporation started at almost the same time. However, the total reduction of evaporation is about 55% of that of the precipitation. The remaining 45% should be contributed by the moisture divergence and changes of the atmospheric condition.

The main moisture source for Sahel summer rainfall is the air flow from the Atlantic Ocean, and for east African, the Indian Ocean. The weakening of the air flows from these two sources would significantly affect the rainfall in the sub–Sahara area. Figure 9 shows the five case mean difference of the wind vectors between desertification and control runs. Since this is a difference map, the vectors there do not necessarily indicate the real wind direction. For example, a westerly wind vector on this map means either the westerlies become stronger, or easterlies become weaker. From Fig. 9, we can find both air flows from Atlantic Ocean and Indian Ocean get weaker and the dry north–east air flows are stronger. This leads to a reduction of the moisture convergence.

Ground temperature just increased slightly in Case D despite of the fact that the latent heat release reduced significantly during the whole period. The decrease of the evaporation is balanced by the changes of the net long wave radiation and short wave radiation absorbed at ground surface.

The time series of short wave radiation absorbed at ground for Cases C2 and D2 are showed in Fig. 10. The net short wave radiation decreased during almost all 90 days in Case D2. The albedo plays a critical role in this effect, despite the fact that the reduced cloud cover (Fig. 11) tended to let more short wave reach the ground. Only when the cloud cover reduced about 0.1, the two cases might receive almost the same amount of short wave radiation.

The changes in sensible heat appeared to be more complex. It was found that in Case D2 it reduced during the first 35 days, then increased slightly during the remaining time period. However, in most other cases, the sensible heat did not increase after it decreased during first 30 days. The simulated outgoing long wave radiation at the top of the atmosphere reduced after desertification.

7. SUMMARY

The rainfall anomaly pattern from our desertification experiment show that the physical processes through which land surface affects the atmosphere are reasonable and consistent with early studies. We showed that the land surface effect might play an important role in the Sahel drought.

8. REFERENCES

Charney, J. G., 1975: Dynamics of deserts and drought in the Sahel. *J. Roy. Meteo. Soc.*, 101, 192–202.

Dregne, H. E., 1977: Desertification of arid lands, economic geography, 53, 322–331.

Hou, Y.-T., 1990: Cloud–radiation–dynamics interaction. Ph.D. dissertation, University of Maryland, 209 pp.

Kinter III, J. L., J. Shukla, L. Marx and E.K. Schneider, 1988: A simulation of the winter and summer circulations with the NMC global spectral model. *J. Atmos. Sci.*, 45, 2486–2522.

Lamb, P. J., 1985: Rainfall in sub–Saharan west Africa during 1941–183. Proceedings of the Third Conference on Climate Variations and Symposium on Contemporary Climate 1850–2100, Los Angeles, 64–67.

Lanly, J. P., 1982: Tropical forest resources. *FAO Forestry Paper*, 30, Rome, 106 pp.

Nicholson, S. E., 1980: The nature of rainfall fluctuations in subtropical west Africa. *Mon. Wea. Rev.*, 108, 473–487.

Nicholson, S. E., 1981: Rainfall and atmospheric circulation during drought periods and wetter years in west Africa. *Mon. Wea. Rev.*, 109, 2191–2208.

Sela, J. G., 1980: Spectral modeling at the National Meteorological Center. *Mon. Wea. Rev.*, 108, 1279–1292.

Sellers, P.J., Y. Mintz, Y.C. Sud and A. Dalcher, 1986: A simple biosphere model (SiB) for use within general circulation models. *J. Atmos. Sci.*, 43, 505–531.

Shukla, J. and Y. Mintz, 1982: A study of the influence of land–surface evapotranspiration on the earth's climate. *Science*, 215, 1498–1501.

Skoupy, J., 1987: Desertification in Africa. *Agric. Met. Prog.*, Proc. Reg. Train. Sem. on Drought and Desertification in Africa. Addis Ababa, 33–45, Geneva, WMO.

Slingo, J. M., 1987: The development and verification of a cloud prediction scheme for the ECMWF model. *Quart. J. Roy. Meteo. Soc.*, 113, 899–927.

Sud, Y. C. and W. E. Smith, 1985: The influence of the surface roughness of deserts on the July circulation. *Bound. Lay. Meteor.*, 33, 15–49.

Walker, J. and P.R. Rowntree, 1977: The effect of soil moisture on circulation and rainfall in a tropical model. *Quart.J.Roy.Meteor.Soc.*, 103, 29–43.

Xue, Y., K. N. Liou and A. Kasahara, 1990: Investigation of biogeophysical feedback on the Africa climate using a two–dimensional model. 3, 338–352.

Xue, Y., P. J. Sellers, J. Kinter and J. Shukla, 1991: A simplified biosphere model for global climate studies. *J. Climate*, 3, 345–364.

TABLE 1

		Type 6	Type 8	Type 9	Type 11
Vegetation cover		0.3	0.1	0.1	0
Leaf area index		2.6	0.26	0.17	0
Greenness		0.87	0.57	0.57	0
Surface roughness(m)		0.93	0.20	0.06	0.01
Soil depth(m)	D1	0.02	0.02	0.02	0.02
	D2	1.48	0.47	0.47	0.17
	D3	2.0	1.0	1.0	0.3
Soil wetness exponent		7.12	4.05	4.05	4.05
Soil tension at saturation(m)		–0.086	–0.035	–0.035	–0.035
Hydraulic conductivity at saturation (m/s)		0.2E–4	0.176E–3	0.176E–3	0.176E–3

TABLE 2

	Initial Condition	SST
1. Control run		
C1	June 1, 1988	Climatology
C2	June 2, 1988	Climatology
C3	June 1, 1987	Climatology
C4	June 1, 1988	1983 SST
C5	June 1, 1988	1950 SST
2. Desertification		
D1	June 1, 1988	Climatology
D2	June 2, 1988	Climatology
D3	June 1, 1987	Climatology
D4	June 1, 1988	1983 SST
D5	June 1, 1988	1950 SST
3. Afforestation		
A1	June 1, 1988	Climatology
A2	June 2, 1988	Climatology
A3	June 1, 1987	Climatology
A4	June 1, 1988	1983 SST
A5	June 1, 1988	1950 SST

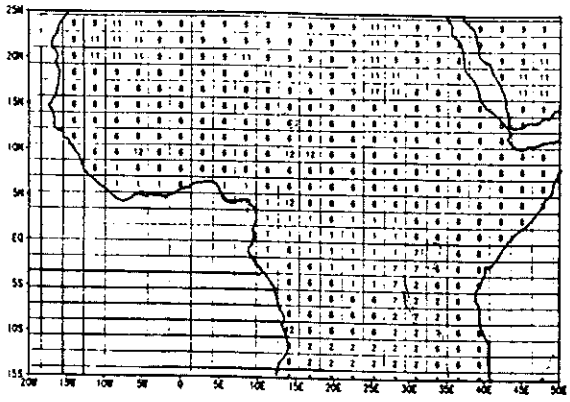

Figure 1a: Vegetation type map for control run.

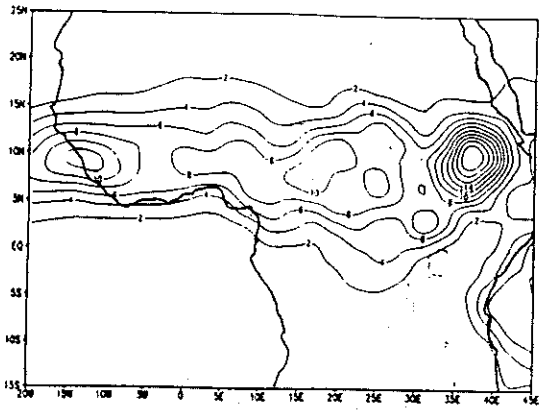

Figure 2a: Ninety day mean precipitation of desertification from five case mean. Contour interval is 2 mm/day.

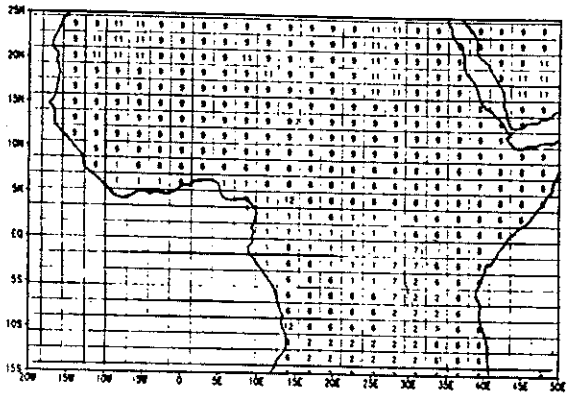

Figure 1b: Vegetation type map for desertification run.

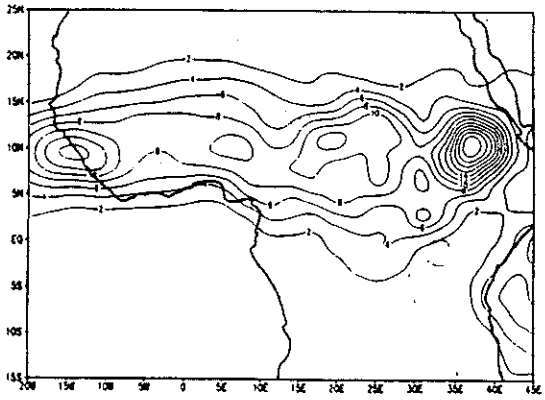

Figure 2b: Ninety day mean precipitation of control from five case mean. Contour interval is 2 mm/day.

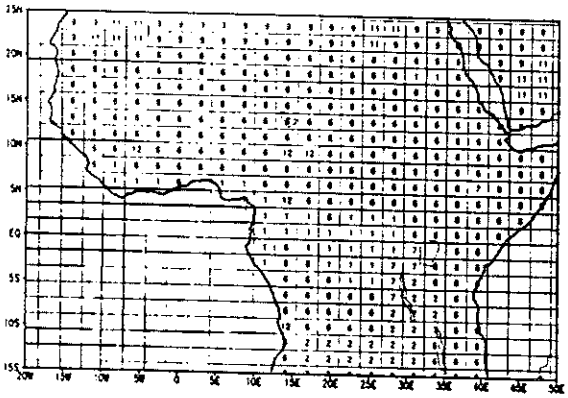

Figure 1c: Vegetation type map for afforestation run.

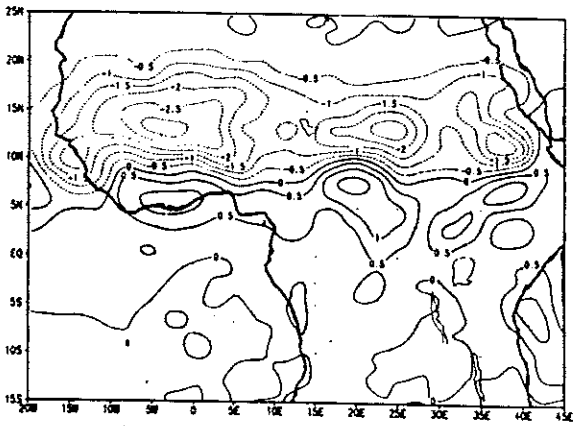

Figure 2c: Ninety day mean precipitation of desertification minus control from five case mean. Contour interval is 0.5 mm/day.

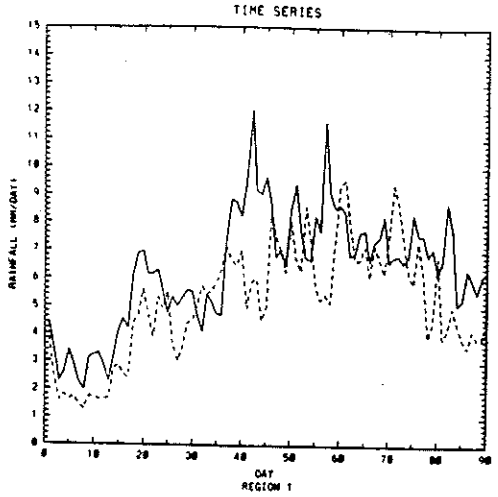

Figure 3: Time series of rainfall of Case C2 and D2 at desertification area.

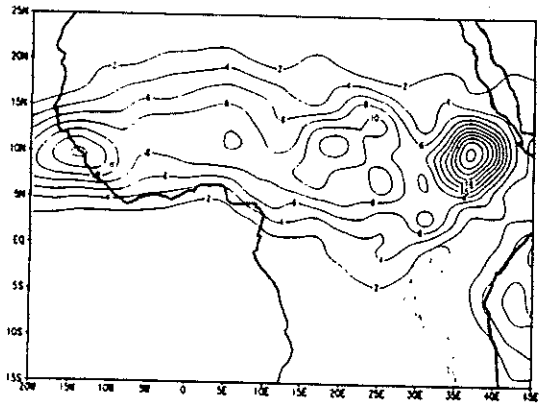

Figure 4a: Ninety day mean precipitation of afforestation from five case mean. Contour interval is 2 mm/day.

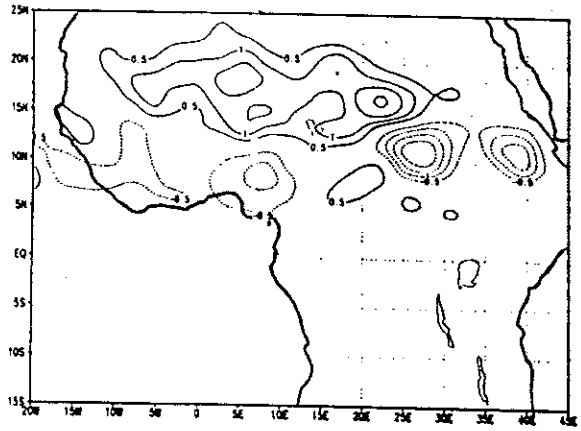

Figure 4b: Ninety day mean precipitation of afforestation minus control from five case mean. Contour interval is 0.5 mm/day.

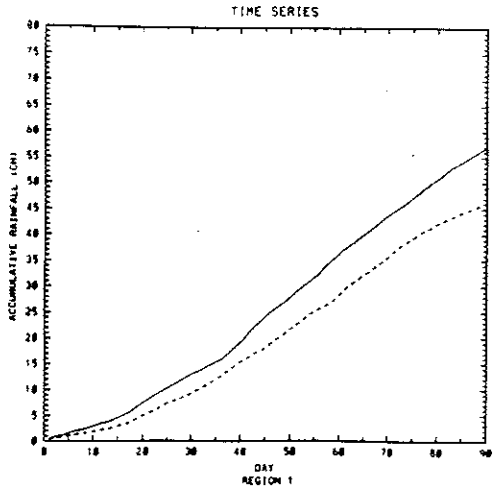

Figure 5: Accumulative rainfall of Case C2 and D2 during 90 days at desertification area.

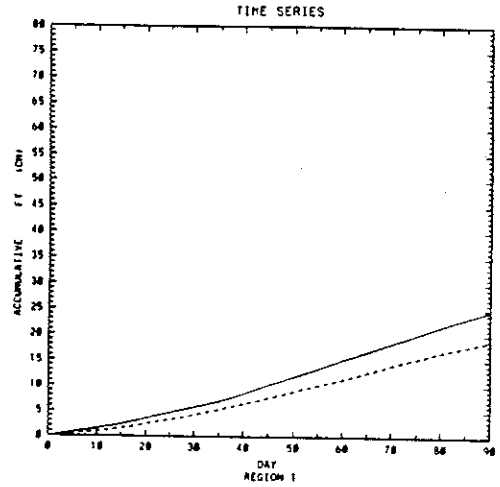

Figure 6: Accumulative evaporation for Case D2 and Case C2.

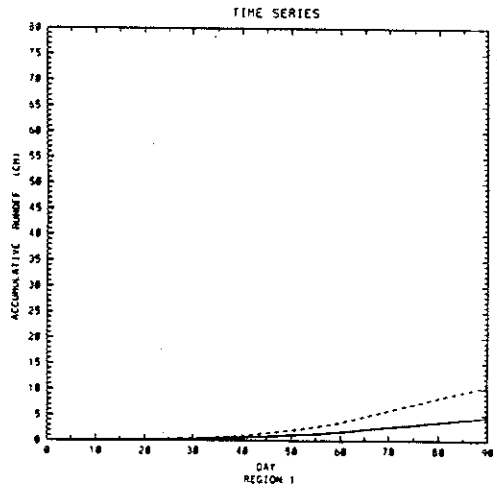

Figure 7: Accumulative runoff for Case D2 and Case C2.

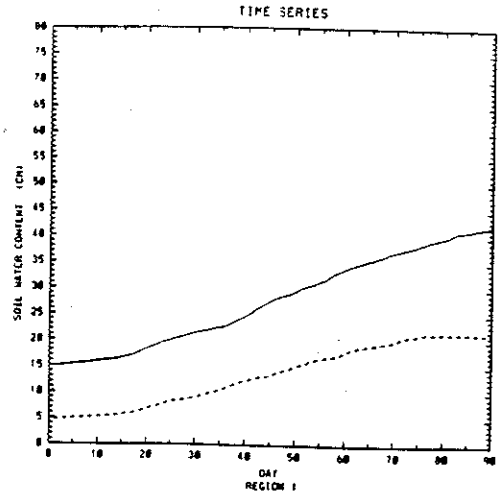

Figure 8: Time series of soil water content of Case C2 and D2 at desertification area.

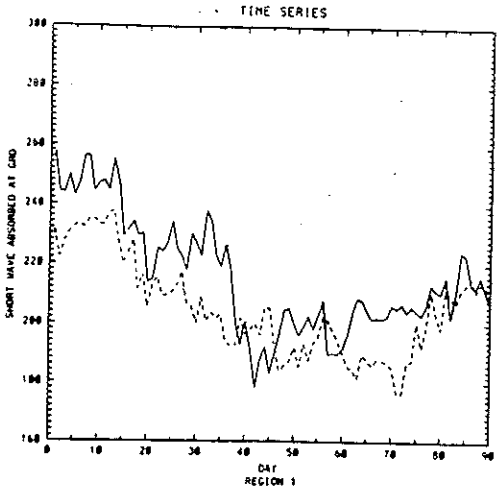

Figure 10: Time series of short wave absorbed at ground for Case D2 and Case C2.

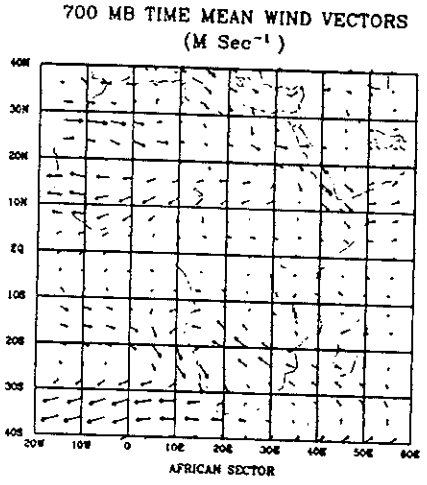

Figure 9: Ninety day mean of wind vector differences of five case mean at 700 mb. Case D minus Case C.

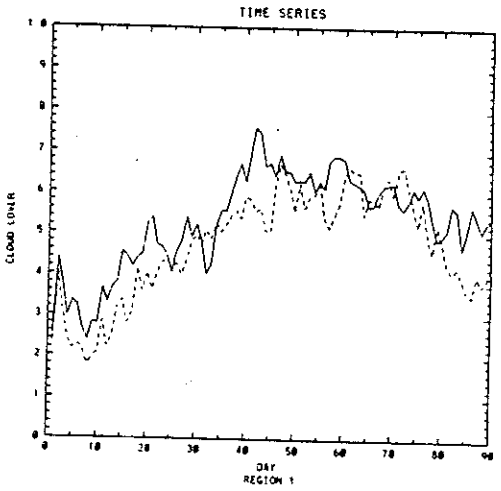

Figure 11: Time series of cloud cover for Case D2 and Case C2.